Please cite this article in press as: Sato et al., The Adipocyte-Inducible Secreted Phospholipases PLA2G5 and PLA2G2E Play Distinct Roles in Obesity, Cell Metabolism (2014), http://dx.doi.org/10.1016/j.cmet.2014.05.002

Cell Metabolism
Article

The Adipocyte-Inducible Secreted Phospholipases PLA2G5 and PLA2G2E Play Distinct Roles in Obesity

Hiroyasu Sato,[1,2] Yoshitaka Taketomi,[1,2] Ayako Ushida,[1,3] Yuki Isogai,[1,3] Takumi Kojima,[1] Tetsuya Hirabayashi,[1] Yoshimi Miki,[1,2] Kei Yamamoto,[1] Yasumasa Nishito,[4] Tetsuyuki Kobayashi,[3] Kazutaka Ikeda,[5] Ryo Taguchi,[6] Shuntaro Hara,[2] Satoshi Ida,[7] Yuji Miyamoto,[7] Masayuki Watanabe,[7] Hideo Baba,[7] Keishi Miyata,[8] Yuichi Oike,[8] Michael H. Gelb,[9] and Makoto Murakami[1,10,*]

[1]Lipid Metabolism Project, Tokyo Metropolitan Institute of Medical Science, 2-1-6 Kamikitazawa, Setagaya-ku, Tokyo 156-8506, Japan
[2]Department of Health Chemistry, Showa University, School of Pharmacy, 1-5-8 Hatanodai, Shinagawa-ku, Tokyo 142-8555, Japan
[3]Department of Biology, Faculty of Science, Ochanomizu University, 2-1-1 Otsuka, Bunkyo-ku, Tokyo 112-8610, Japan
[4]Core Technology and Research Center, Tokyo Metropolitan Institute of Medical Science, 2-1-6 Kamikitazawa, Setagaya-ku, Tokyo 156-8506, Japan
[5]Institute for Advanced Biosciences, Keio University, 246-2 Mizukami, Kakuganji, Tsuruoka, Yamagata 997-0052, Japan
[6]Department of Biomedical Sciences, College of Life and Health Sciences, Chubu University, 1200 Matsumoto-cho, Kasugai-shi, Aichi 487-8501, Japan
[7]Department of Gastroenterological Surgery, Kumamoto University, 1-1-1 Honjo, Chuo-ku, Kumamoto 860-8556, Japan
[8]Department of Molecular Genetics, Kumamoto University, 1-1-1 Honjo, Chuo-ku, Kumamoto 860-8556, Japan
[9]Departments of Chemistry and Biochemistry, University of Washington, Campus Box 351700, 36 Bagley Hall, Seattle, WA 98195, USA
[10]CREST, Japan Science and Technology Agency, 4-1-8 Honcho, Kawaguchi, Saitama 332-0012, Japan
*Correspondence: murakami-mk@igakuken.or.jp
http://dx.doi.org/10.1016/j.cmet.2014.05.002

SUMMARY

Metabolic disorders, including obesity and insulin resistance, have their basis in dysregulated lipid metabolism and low-grade inflammation. In a microarray search of unique lipase-related genes whose expressions are associated with obesity, we found that two secreted phospholipase A_2s ($sPLA_2$s), PLA2G5 and PLA2G2E, were robustly induced in adipocytes of obese mice. Analyses of *Pla2g5*$^{-/-}$ and *Pla2g2e*$^{-/-}$ mice revealed distinct roles of these $sPLA_2$s in diet-induced obesity. PLA2G5 hydrolyzed phosphatidylcholine in fat-overladen low-density lipoprotein to release unsaturated fatty acids, which prevented palmitate-induced M1 macrophage polarization. As such, PLA2G5 tipped the immune balance toward an M2 state, thereby counteracting adipose tissue inflammation, insulin resistance, hyperlipidemia, and obesity. PLA2G2E altered minor lipoprotein phospholipids, phosphatidylserine and phosphatidylethanolamine, and moderately facilitated lipid accumulation in adipose tissue and liver. Collectively, the identification of "metabolic $sPLA_2$s" adds this gene family to a growing list of lipolytic enzymes that act as metabolic coordinators.

INTRODUCTION

Type 2 diabetes and metabolic syndrome are increasing at an explosive rate worldwide due to a pandemic of obesity associated with insulin resistance, nonalcoholic fatty liver disease, and hyperlipidemia (Després and Lemieux, 2006). The mechanisms connecting obesity to insulin resistance include an elevation of circulating lipids, ectopic lipid deposition leading to lipotoxicity, and chronic inflammation in metabolically active tissues (Hotamisligil, 2006). Obesity relies on dysregulations of intracellular lipid metabolism or extracellular lipid partitioning among tissues, and perturbation of intracellular/extracellular lipases or related enzymes variably and often profoundly affect obesity and insulin resistance (Chen et al., 2008; Chiu et al., 2010; Haemmerle et al., 2006; Jaworski et al., 2009; Tian et al., 2010; Wang et al., 2011).

Among the phospholipase A_2 (PLA_2) family, secreted PLA_2s ($sPLA_2$s) have been implicated in inflammation and atherosclerosis, since they can augment the production of proinflammatory lipid mediators and hydrolyze phospholipids in lipoproteins to generate proatherogenic particles in vitro (Murakami et al., 2011). Recent genetic studies have revealed that individual $sPLA_2$s, which show distinct tissue distributions and substrate preferences, participate in diverse biological events in response to given microenvironmental cues (Sato et al., 2010; Taketomi et al., 2013). However, the regulatory roles of $sPLA_2$s in metabolic disorders are not well understood. Except for studies using $sPLA_2$-overexpressing transgenic mice (Ivandic et al., 1999; Sato et al., 2008), no reports have firmly established whether $sPLA_2$s could affect lipoprotein metabolism in vivo. Moreover, although $sPLA_2$s exert anti-inflammatory effects in certain situations (Ait-Oufella et al., 2013; Miki et al., 2013), except for PLA2G2D (group IID), a "resolving $sPLA_2$" that ameliorates inflammation by mobilizing proresolving lipid mediators (Miki et al., 2013), the molecular mechanisms for the anti-inflammatory actions of $sPLA_2$s remain elusive.

In our efforts to search for particular lipase-related genes whose roles in obesity have not been addressed before, we found that two particular $sPLA_2$s, PLA2G5 (group V) and PLA2G2E (group IIE), were robustly induced in adipose tissue of obese mice. Reportedly, PLA2G5 deficiency exacerbates or

Please cite this article in press as: Sato et al., The Adipocyte-Inducible Secreted Phospholipases PLA2G5 and PLA2G2E Play Distinct Roles in Obesity, Cell Metabolism (2014), http://dx.doi.org/10.1016/j.cmet.2014.05.002

attenuates inflammation according to disease contexts in unknown ways (Murakami et al., 2011). Notably, *PLA2G5* gene polymorphisms correlate with low-density lipoprotein (LDL) levels in subjects with type 2 diabetes or obesity (Sergouniotis et al., 2011; Wootton et al., 2007), and in vitro PLA2G5 susceptibility of LDL from patients with type 2 diabetes is greater than that of LDL from healthy subjects (Pettersson et al., 2008), suggesting a role of this $sPLA_2$ in metabolic regulation. After the identification of PLA2G2E (Suzuki et al., 2000; Valentin et al., 1999), its expression, target phospholipids, and biological roles in vivo have remained a mystery for more than a decade. We now provide evidence that the two diet-inducible, adipocyte-driven "metabolic $sPLA_2$s" play distinct roles in obesity, hyperlipidemia, and insulin resistance, thus highlighting the importance of the $sPLA_2$ family in lipoprotein hydrolysis and immune regulation in the process of metabolic disorders.

RESULTS

PLA2G5 and PLA2G2E Are Induced in Adipocytes of Obese Mice

We performed gene profiling by microarray followed by quantitative RT-PCR of perigonadal white adipose tissue (WAT) from C57BL/6 mice fed a high-fat diet (HFD; 60% fat calorie) in comparison with those maintained on a low-fat diet (LFD; 4.8% fat calorie) to identify particular lipase-related genes whose expression levels were altered by diets and whose functions in obesity are currently unknown. We found that *Pla2g5* and *Pla2g2e*, two members of the $sPLA_2$ family, were highly induced in the WAT of HFD-fed mice compared with LFD-fed mice, ranking two of the top three among the diet-inducible lipase-related genes (Figure 1A; Table S1, available online). Marked induction of these two $sPLA_2$s, but not other $sPLA_2$s (Figure 1B) and intracellular PLA_2s (Figure S1A), in the WAT of HFD-fed mice was confirmed by quantitative PCR. As in mice, the expression of *PLA2G5* was much higher than that of most other $sPLA_2$s in human mesenteric WAT and fatty appendices, while that of *PLA2G2E* was very low (Figure 1C; Table S2). Note that PLA2G2A, which is highly homologous to PLA2G2E (Suzuki et al., 2000; Valentin et al., 1999) and absent in C57BL/6 mice due to a natural mutation (MacPhee et al., 1995), was highly expressed in human WAT, suggesting that PLA2G2E in mice might be compensated by PLA2G2A in humans.

Among the tissues with high lipid demand, constitutive *Pla2g5* expression in heart and skeletal muscle was unaffected by diet, and its expression in WAT of HFD-fed mice exceeded that in any other tissues examined so far and reached a level much higher than that in bone marrow (BM)-derived denditic cells (BMDCs) and macrophages (BMDMs) (Figure 1D). HFD-induced expression of *Pla2g2e* occurred robustly in WAT and brown adipose tissue (BAT), while its expression in other tissues and cells was low (Figure 1E). Moreover, WAT expression of both $sPLA_2$s was far greater in genetically obese $Lep^{ob/ob}$ mice than in control mice (Figure 1F). Kinetic experiments after HFD feeding revealed robust induction of *Pla2g5* and *Pla2g2e* in WAT by 8 weeks, thereafter reaching a maximal plateau level (Figure S1A). The kinetic induction of *Pla2g5* and *Pla2g2e* was similar to that of *Lep*, which encodes leptin (Pelleymounter et al., 1995), but differed from that of adipogenic or immune cell markers (Figure S1A). More detailed kinetic studies at an earlier period showed that the HFD induction of *Pla2g2e* preceded that of *Pla2g5* (Figure S1B). When the WAT was separated into adipocytes and stromal vascular fraction (SVF), both $sPLA_2$s were located predominantly in adipocytes of HFD-fed mice (Figures 1G and S1C).

Expression of *Pla2g5* and *Pla2g2e* was increased markedly in mouse 3T3-L1 preadipocytes after culture for 14 days with an adipogenic cocktail (Figure S1D). Proinflammatory cytokines failed to affect their expression in 3T3-L1 cells (Figure S1E). Transwell culture of SVF cells and 3T3-L1 cells did not affect or even decreased the expression of *Pla2g5* and *Pla2g2e*, while it increased that of *Tnf* and *Ccl2*, in the latter cells (Figure S1F), ruling out the contribution of SVF-derived soluble factors to the induction of these $sPLA_2$s in adipocytes. Notably, *Pla2g5*, not *Pla2g2e*, expression in differentiated 3T3-L1 cells was further increased by the endoplasmic reticulum (ER) stress inducer thapsigargin (Figure S1D) or tunicamycin (data not shown). These results suggest that the inducible expression of *Pla2g5* depends on the adipogenic program plus obesity-associated ER stress (Ozcan et al., 2006), while adipogenesis is sufficient to drive *Pla2g2e* expression. During adipogenesis, *Pla2g2e* expression started to increase on day 3, lagging behind the induction of the adipogenic marker *Pparg*, and continued to increase by day 12 (Figure S1G).

Increased Diet-Induced Obesity in *Pla2g5*$^{-/-}$ Mice

To elucidate the role of PLA2G5 in obesity, we placed $Pla2g5^{-/-}$ mice (Satake et al., 2004) and wild-type (WT) littermates on a HFD, along with a control group of each genotype on a LFD. HFD-induced obesity and weight gain were greater in $Pla2g5^{-/-}$ mice than in $Pla2g5^{+/+}$ mice (Figures 2A and 2B). Immunohistochemistry confirmed the location of PLA2G5 protein in adipocytes of HFD-fed WT mice, whereas hardly any such reactivity was seen in those of $Pla2g5^{-/-}$ mice, which lacked *Pla2g5* expression (Figures S2A and S2B). Computed tomography (CT) showed significant increases in total, visceral, and subcutaneous fat depositions in HFD-fed $Pla2g5^{-/-}$ mice relative to $Pla2g5^{+/+}$ mice (Figure 2C). In agreement, the HFD-induced increase in plasma leptin, whose expression correlates with adiposity (Pelleymounter et al., 1995), was higher in $Pla2g5^{-/-}$ mice than in $Pla2g5^{+/+}$ mice (Figure 2D). Although daily food intake was the same for both groups, locomotion and oxygen consumption were lower in $Pla2g5^{-/-}$ mice (Figures S2C–S2E), indicating decreased energy expenditure. The respiratory quotient was unchanged in $Pla2g5^{-/-}$ mice (Figure S2F).

HFD-induced elevation of plasma insulin was greater in $Pla2g5^{-/-}$ mice than in $Pla2g5^{+/+}$ mice (Figure 2E), despite comparable hyperglycemia in both genotypes (Figure S2G), suggesting exacerbated insulin resistance in $Pla2g5^{-/-}$ mice. Indeed, on an insulin tolerance test (ITT), HFD-fed $Pla2g5^{-/-}$ mice had greater insulin resistance than $Pla2g5^{+/+}$ mice (Figure 2F). Insulin-stimulated Akt phosphorylation was lower in WAT, but not in skeletal muscle and liver, of $Pla2g5^{-/-}$ mice than in that of $Pla2g5^{+/+}$ mice (Figures 2G and S2H), suggesting that *Pla2g5* ablation decreases insulin sensitivity mainly in WAT, where PLA2G5 is induced. In a glucose tolerance test (GTT), the glucose disposal was similar in both genotypes (Figure 2H), probably because glucose-stimulated insulin secretion was greater in $Pla2g5^{-/-}$ mice than in $Pla2g5^{+/+}$ mice (Figure 2I).

Please cite this article in press as: Sato et al., The Adipocyte-Inducible Secreted Phospholipases PLA2G5 and PLA2G2E Play Distinct Roles in Obesity, Cell Metabolism (2014), http://dx.doi.org/10.1016/j.cmet.2014.05.002

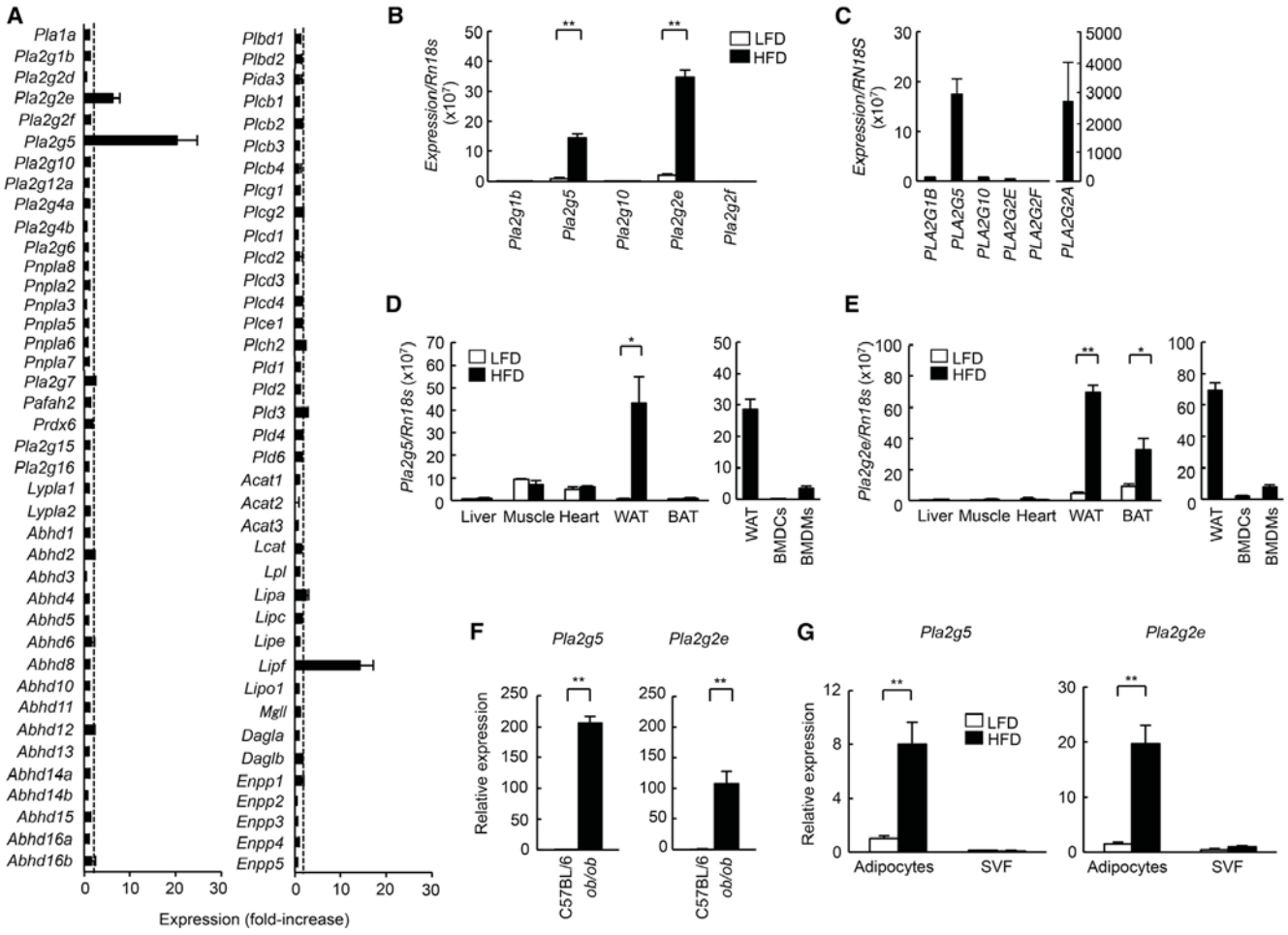

Figure 1. Obesity-Induced Expression of *Pla2g5* and *Pla2g2e* in Hypertrophic Adipocytes

(A) Microarray of lipase-related genes in the WAT of C57BL/6 mice fed a LFD or HFD for 18 weeks. Values indicate fold increases in the HFD group relative to the LFD group (n = 4; mean ± SD).

(B) Expression of sPLA$_2$ mRNAs relative to *Rn18s* in the WAT of C57BL/6 mice fed a LFD (n = 6) or HFD (n = 9).

(C) Expression of sPLA$_2$ mRNAs relative to *RN18S* in human visceral WAT (n = 18).

(D and E) Expression of *Pla2g5* (D) and *Pla2g2e* (E) in various tissues and cells of C57BL/6 mice (n = 5).

(F) Expression of *Pla2g5* and *Pla2g2e* in WAT of 12-week-old *Lep*$^{ob/ob}$ mice, the expression in age-matched C57BL/6 mice being regarded as 1 (n = 3).

(G) *Pla2g5* and *Pla2g2e* expression in adipocytes and SVF from WAT of LFD- or HFD-fed mice, the expression in adipocytes from LFD-fed mice being regarded as 1 (n = 8).

In (B), (D), (E), and (G), mice were fed a LFD or HFD for 26 weeks. Data are compiled from one (A, C, and F) or two (B, D, E, and G) experiments. Mean ± SEM (B–G), *$p < 0.05$, **$p < 0.01$.

Exacerbated insulin resistance was already evident, whereas oxygen consumption was unaffected, in *Pla2g5*$^{-/-}$ mice at 6 weeks after HFD feeding (Figures S2I and S2J), indicating that the metabolic dysfunction occurred prior to the decreased energy expenditure.

HFD feeding led to greater adipocyte hypertrophy in WAT (Figure 2J) and BAT (Figure S3A) of *Pla2g5*$^{-/-}$ mice compared to those of WT mice, although expression levels of adipogenic, lipogenic, lipid uptake, lipolytic, or thermogenic genes in WAT (Figure 2K) and BAT (Figure S3B) were similar between the genotypes. Expression of several other PLA$_2$s, which have been implicated in adiposity (Su et al., 2004), in WAT was unaffected by PLA2G5 deficiency (Figure S3C). Thus, the increased obesity in *Pla2g5*$^{-/-}$ mice may not arise from intrinsic alterations in these adipocyte programs but may involve other extrinsic mechanisms. HFD-increased plasma alanine aminotransferase (ALT) level (Figure 2L) and hepatic fat deposition (Figures 2M and 2N) were greater in *Pla2g5*$^{-/-}$ mice compared to *Pla2g5*$^{+/+}$ mice. Consistently, hepatic expression of genes for lipid synthesis or uptake and inflammation, but not for β-oxidation, was increased in HFD-fed *Pla2g5*$^{-/-}$ mice over *Pla2g5*$^{+/+}$ mice (Figures S3D and S3E), indicating exacerbated hepatic steatosis in *Pla2g5*$^{-/-}$ mice. Since the expression of *Pla2g5* in BAT and liver was low (Figure 1D), and since visceral adiposity and hepatic steatosis are etiologically intertwined (Després and Lemieux, 2006), the abnormalities in these tissues may reflect a secondary effect resulting from the increased obesity in *Pla2g5*$^{-/-}$ mice.

Please cite this article in press as: Sato et al., The Adipocyte-Inducible Secreted Phospholipases PLA2G5 and PLA2G2E Play Distinct Roles in Obesity, Cell Metabolism (2014), http://dx.doi.org/10.1016/j.cmet.2014.05.002

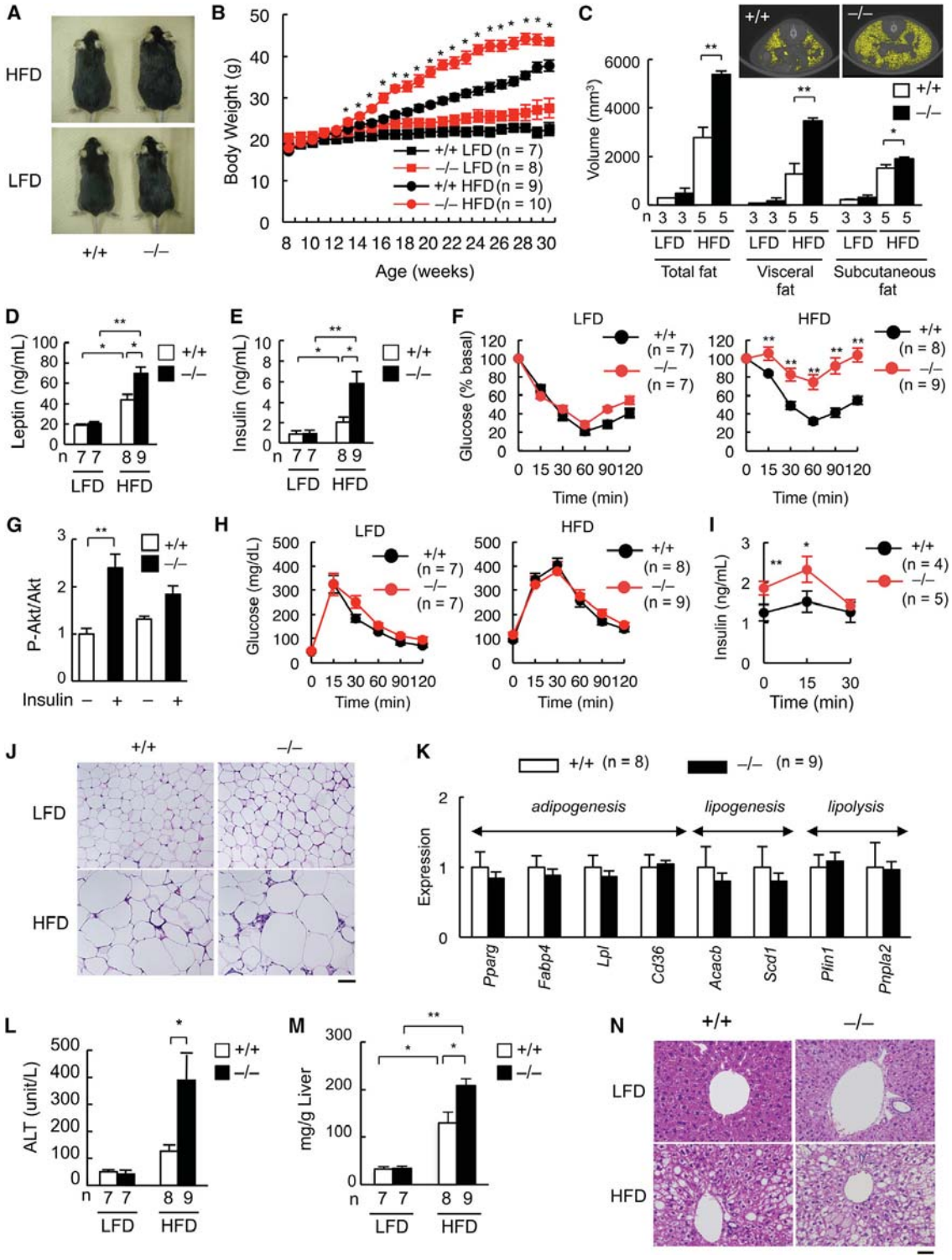

Figure 2. Increased Diet-Induced Obesity in *Pla2g5*$^{-/-}$ Mice

(A) Representative photos of *Pla2g5*$^{+/+}$ and *Pla2g5*$^{-/-}$ mice fed a LFD or HFD for 14 weeks.

(B) Body weights of *Pla2g5*$^{+/+}$ and *Pla2g5*$^{-/-}$ mice placed on a LFD or HFD for the indicated periods.

(C) CT analysis of fat volumes in *Pla2g5*$^{+/+}$ and *Pla2g5*$^{-/-}$ mice. Yellow areas indicate fat deposition in HFD-fed mice (inset).

(D and E) Levels of fasting plasma leptin (D) and insulin (E) in *Pla2g5*$^{+/+}$ and *Pla2g5*$^{-/-}$ mice.

(F) ITT using 6 hr fasted *Pla2g5*$^{+/+}$ and *Pla2g5*$^{-/-}$ mice.

(G) Immunoblotting of phosphorylated (P-) and total Akt in WAT of HFD-fed *Pla2g5*$^{+/+}$ and *Pla2g5*$^{-/-}$ mice with (+) or without (–) 5 min treatment with insulin. The ratios of P-Akt to Akt were determined by densitometry, with the value of insulin-untreated *Pla2g5*$^{+/+}$ mice being regarded as 1 (n = 4).

(legend continued on next page)

Please cite this article in press as: Sato et al., The Adipocyte-Inducible Secreted Phospholipases PLA2G5 and PLA2G2E Play Distinct Roles in Obesity, Cell Metabolism (2014), http://dx.doi.org/10.1016/j.cmet.2014.05.002

Altered Lipoprotein Profiles in HFD-Fed *Pla2g5*$^{-/-}$ Mice

PLA2G5 hydrolyzes phosphatidylcholine (PC) in LDL and, to a lesser extent, in high-density lipoprotein (HDL) in vitro (Sato et al., 2008), yet in vivo evidence for this action was lacking. Kinetically, HFD feeding was accompanied by increases of phospholipids in plasma and in lipoproteins (Figure S4A), which preceded *Pla2g5* induction in WAT (Figure S1A). Plasma phospholipid and cholesterol levels were significantly greater in HFD-fed *Pla2g5*$^{-/-}$ mice than in *Pla2g5*$^{+/+}$ mice (Figure 3A). Moreover, phospholipid, cholesterol, and TG levels in LDL, but not chylomicron (CM), very-low-density lipoprotein (VLDL), and HDL, were significantly higher in HFD-fed *Pla2g5*$^{-/-}$ mice than in *Pla2g5*$^{+/+}$ mice (Figures 3B–3D, S4B, and S4C). These results suggest that diet-induced PLA2G5 acts on LDL phospholipids, eventually altering LDL lipid composition.

To explore the hydrolysis of LDL phospholipids by PLA2G5 further, phospholipids in LDL from HFD-fed mice were analyzed by electrospray ionization mass spectrometry (ESI-MS). LDL in HFD-fed *Pla2g5*$^{-/-}$ mice contained more PC34:1 (*sn*-1 palmitic acid [PA; 16:0] and *sn*-2 oleic acid [OA; 18:1])—and, to a lesser extent, other PC species containing polyunsaturated fatty acids (PUFAs), such as PC34:2 (16:0 and linoleic acid [LA; 18:2]), PC36:3 (18:1 and 18:2), PC36:4 (16:0 and arachidonic acid [AA; 20:4]), and PC38:6 (16:0 and docosahexaenoic acid [DHA, 22:6])—than that in *Pla2g5*$^{+/+}$ mice (Figures 3E and S4D). By contrast, PLA2G5 deficiency did not affect minor LDL phospholipids, phosphatidylethanolamine (PE), and phosphatidylserine (PS) (Figure 3E). These results imply that PLA2G5 preferentially hydrolyzes PC species (particularly those containing a fatty acid with a lower degree of unsaturation, such as OA in preference to LA [OA > LA]) in hyperlipidemic LDL in vivo, a view that agrees with its substrate preference in vitro (Pruzanski et al., 2005; Sato et al., 2008). Plasma levels of nonesterified fatty acids (NEFA) and lysophosphatidylcholine (LPC), which are PLA$_2$ reaction products, did not differ in both genotypes (Figure S4E), probably because the PLA2G5-driven NEFA and LPC pools were small relative to their high background levels or because they were produced locally in WAT. In support of the latter idea, the WAT level of OA was elevated in *Pla2g5*$^{+/+}$ mice after HFD feeding, whereas this increase was not seen in *Pla2g5*$^{-/-}$ mice (Figure 3F). PUFAs (LA > AA > DHA) also tended to be lower in HFD-fed *Pla2g5*$^{-/-}$ mice than in *Pla2g5*$^{+/+}$ mice, though to a lesser extent than OA. Overall, these lipid profiles agree with the fatty acid preference of PLA2G5. Thus, diet-induced PLA2G5 hydrolyzes PC in fat-overladen LDL to provide OA in preference to PUFAs in WAT, which may eventually contribute to LDL lipid normalization. Notably, as in mice, WAT expression levels of *PLA2G5* showed a significantly inverse correlation with plasma LDL levels in humans (Figure 3G; Table S2), revealing an enzyme-substrate relationship across species.

Exacerbated Adipose Tissue Inflammation in HFD-Fed *Pla2g5*$^{-/-}$ Mice

Crown-like structures, an indication of macrophage infiltration, were histologically greater in the WAT of HFD-fed *Pla2g5*$^{-/-}$ than in that of *Pla2g5*$^{+/+}$ mice (Figure 2J). Consistently, HFD-induced WAT expression of M1 macrophage markers was increased, whereas M2 macrophage markers were unchanged or decreased, by *Pla2g5* deficiency, allowing the M1/M2 ratio to be greater in HFD-fed *Pla2g5*$^{-/-}$ mice (Figures 4A and 4B). Flow cytometry confirmed that the WAT of HFD-fed *Pla2g5*$^{-/-}$ mice contained a greater proportion of F40/80$^+$CD11b$^+$ macrophages, with a greater number of CD11c$^+$ M1 and fewer CD206$^+$ M2 macrophages, compared to the WAT of *Pla2g5*$^{+/+}$ mice (Figures 4C and 4D). Thus, PLA2G5 plays an anti-inflammatory role in adipose tissue inflammation.

Recruitment of macrophages into obese WAT relies on several mechanisms, among which adipocyte death due to lipotoxicity represents a driving factor, attracting macrophages for phagocytic clearance of dead cells (Cinti et al., 2005). As *Pla2g5*$^{-/-}$ mice display lower macrophage phagocytosis (Balestrieri et al., 2009; Boilard et al., 2010), we evaluated dead cells in *Pla2g5*$^{-/-}$ or *Pla2g5*$^{+/+}$ WAT. TUNEL staining revealed a marked increase of dead cells in WAT of HFD-fed *Pla2g5*$^{-/-}$ mice over *Pla2g5*$^{+/+}$ mice (Figures 4E and 4F). Thus, the reduced clearance of dead cells by macrophages may account, at least partly, for the increased inflammation in *Pla2g5*$^{-/-}$ WAT.

PLA2G5 Integrates Lipoprotein Metabolism and Anti-Inflammation

Given that sPLA$_2$ acts in a paracrine fashion, we speculated that PLA2G5 secreted from adipocytes affected the properties of macrophages. Addition of PLA2G5 to lipopolysaccharide and interferon γ (LPS+IFN-γ)-stimulated BMDMs augmented the expression of the M2 marker *Arg1* without affecting that of the M1 marker *Nos2* (Figure 5A), suggesting that PLA2G5 selectively upregulates the M2 gene. In a setting physiologically more relevant to sterile inflammation in obesity, exposure of BMDMs to PA, a saturated fatty acid that elicits proinflammatory responses through Toll-like receptor 4 (TLR4) or ER stress (Hotamisligil, 2006), increased *Nos2*, did not affect *Arg1*, and decreased *Cd206*, indicative of M1 skewing (Figures 5B and 5C). Further addition of PLA2G5 to PA-treated BMDMs reduced *Nos2*, upregulated *Arg1*, and partially restored *Cd206* expression (Figure 5B). *Pla2g5* expression was increased in PA-treated BMDMs (Figure 5D), in line with its induction by ER stress in adipocytes (Figure S1D). However, culture of *Pla2g5*$^{+/+}$ and *Pla2g5*$^{-/-}$

(H) GTT using 16 hr fasted *Pla2g5*$^{+/+}$ and *Pla2g5*$^{-/-}$ mice.

(I) Glucose-stimulated insulin secretion under the conditions in (H).

(J) Hematoxylin and eosin staining of WAT in *Pla2g5*$^{+/+}$ and *Pla2g5*$^{-/-}$ mice (scale bar, 50 μm).

(K) Expression of adipogenic, lipogenic, and lipolytic genes normalized by *Gapdh* in WAT of HFD-fed *Pla2g5*$^{+/+}$ and *Pla2g5*$^{-/-}$ mice, with the expression in *Pla2g5*$^{+/+}$ mice being regarded as 1.

(L and M) Levels of plasma ALT (L) and hepatic TG (M) in *Pla2g5*$^{+/+}$ and *Pla2g5*$^{-/-}$ mice.

(N) Hematoxylin and eosin staining of liver from *Pla2g5*$^{+/+}$ and *Pla2g5*$^{-/-}$ mice (scale bar, 50 μm).

In (C)–(N), mice were fed a LFD or HFD for 26 weeks. Data are compiled from two (C, G, and I) or three (B, D–F, H, and K–M) experiments. Images in (A), (J), and (N) are representative of two experiments. Mean ± SEM; *$p < 0.05$, **$p < 0.01$.

Please cite this article in press as: Sato et al., The Adipocyte-Inducible Secreted Phospholipases PLA2G5 and PLA2G2E Play Distinct Roles in Obesity, Cell Metabolism (2014), http://dx.doi.org/10.1016/j.cmet.2014.05.002

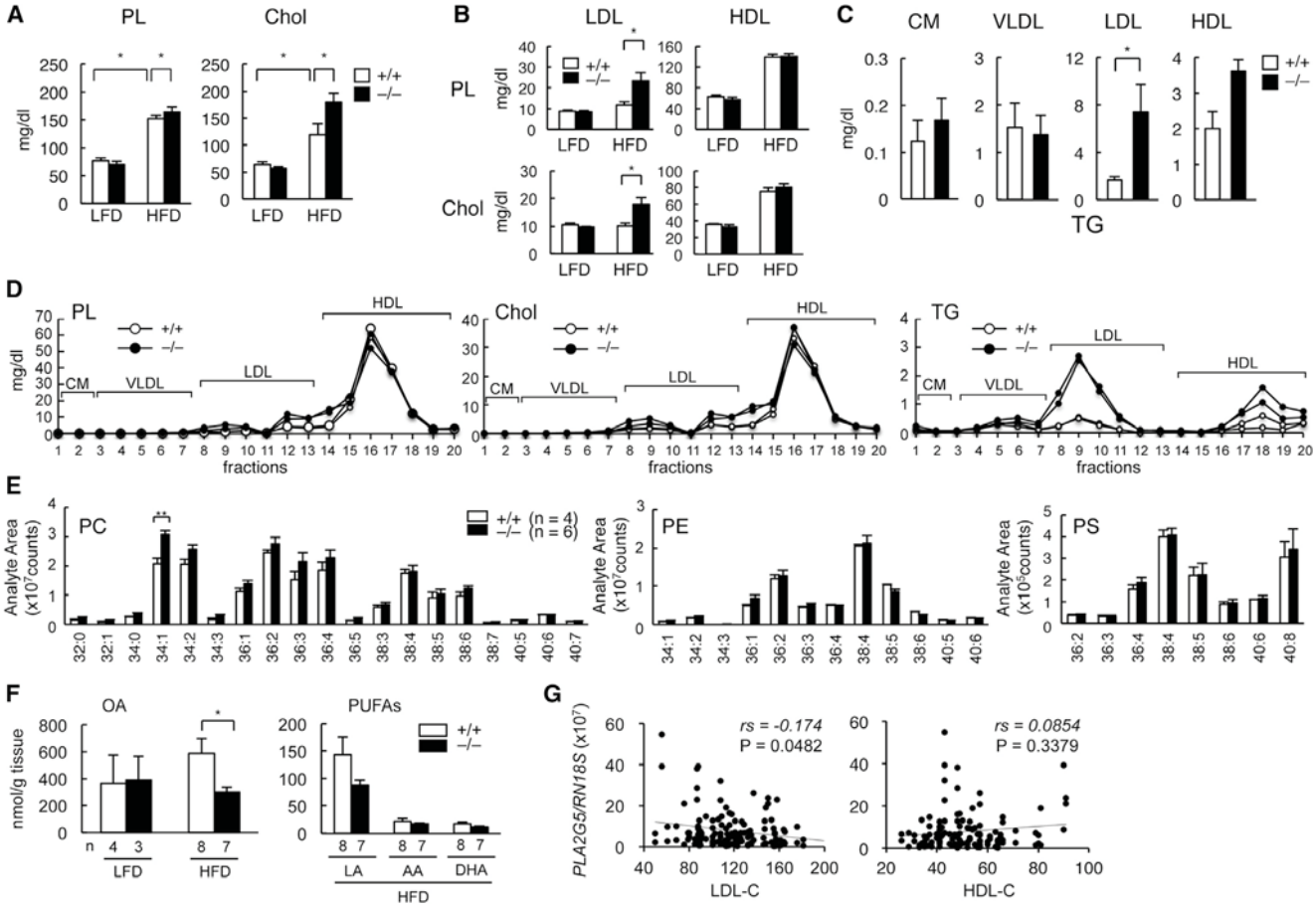

Figure 3. Altered Lipoprotein Profiles in HFD-Fed *Pla2g5*$^{-/-}$ Mice

(A) Plasma phospholipids (PL) and cholesterol (Chol) levels in *Pla2g5*$^{+/+}$ and *Pla2g5*$^{-/-}$ mice (n = 4).

(B) PL and Chol levels in LDL and HDL from *Pla2g5*$^{+/+}$ and *Pla2g5*$^{-/-}$ mice (n = 4).

(C) TG levels in individual lipoprotein particles from HFD-fed *Pla2g5*$^{+/+}$ and *Pla2g5*$^{-/-}$ mice (n = 4).

(D) High-performance liquid chromatography (HPLC) profiles of PL, Chol, and TG in plasma lipoproteins from HFD-fed *Pla2g5*$^{+/+}$ and *Pla2g5*$^{-/-}$ mice. Two examples from each genotype are shown.

(E) ESI-MS of PC, PE, and PS in LDL from HFD-fed *Pla2g5*$^{+/+}$ and *Pla2g5*$^{-/-}$ mice.

(F) ESI-MS of unsaturated fatty acids in WAT of *Pla2g5*$^{+/+}$ and *Pla2g5*$^{-/-}$ mice.

(G) Correlation of *PLA2G5* expression levels in human visceral WAT with LDL or HDL cholesterol (n = 128, 64 from mesentric WAT and 64 from colorectal fat appendices).

In (A)–(F), mice were fed a LFD or HFD for 26 weeks. Data are representative of (A–C) or compiled from (D–G) two experiments. Mean ± SEM; *p < 0.05, **p < 0.01.

BMDMs under M1 or M2 skewing conditions led to a similar induction of respective macrophage subset markers (Figure S5A), suggesting that although PLA2G5 expressed at a low level in macrophages is insufficient to affect their polarization, it can facilitate the conversion of M1 to M2 macrophages when supplied abundantly through a paracrine route. Indeed, when irradiated WT mice were adoptively transferred with *Pla2g5*$^{-/-}$ or *Pla2g5*$^{+/+}$ BM cells, HFD-induced obesity, insulin resistance, and hyperlipidemia were comparable in both groups (Figures S5B–S5D). Thus, PLA2G5 in nonhematopoietic cells (likely adipocytes) appears to be mainly responsible for the amelioration of metabolic disorders.

Of the potential PLA2G5-driven lipid mediators tested, prostaglandin E_2 (PGE_2), an AA metabolite, had the ability to induce *Arg1*, without affecting *Nos2*, in BMDMs stimulated with LPS+IFN-γ (Figure 5E) or PA (Figure 5F). Exogenous PLA2G5 augmented PGE_2 generation by PA-stimulated BMDMs (Figure 5G). In vivo, however, the WAT level of PGE_2 did not differ between HFD-fed *Pla2g5*$^{-/-}$ and *Pla2g5*$^{+/+}$ mice, while that of PGD_2 was higher in the null mice, likely due to upregulation of PGD_2 synthase (Figures S5E and S5F). Thus, it is more likely that PLA2G5 action involves an alternative lipid-mediated process.

Proinflammatory ER stress induced by saturated fatty acids can be ameliorated by unsaturated fatty acids (Hotamisligil, 2006). As PLA2G5 released OA > LA from LDL-PC (Figures 3D and 3E), we examined whether these unsaturated fatty acids affected PA-induced M1 macrophage polarization. Strikingly, OA or LA canceled out the induction of *Nos2* even at 2 μM and also restored the expression of *Cd206* dose dependently in PA-treated BMDMs (Figure 5H). The WAT level of the PLA2G5-sensitive OA pool was within a range enough to affect macrophage polarization (Figures 3E and 5H). Thus, OA, and possibly

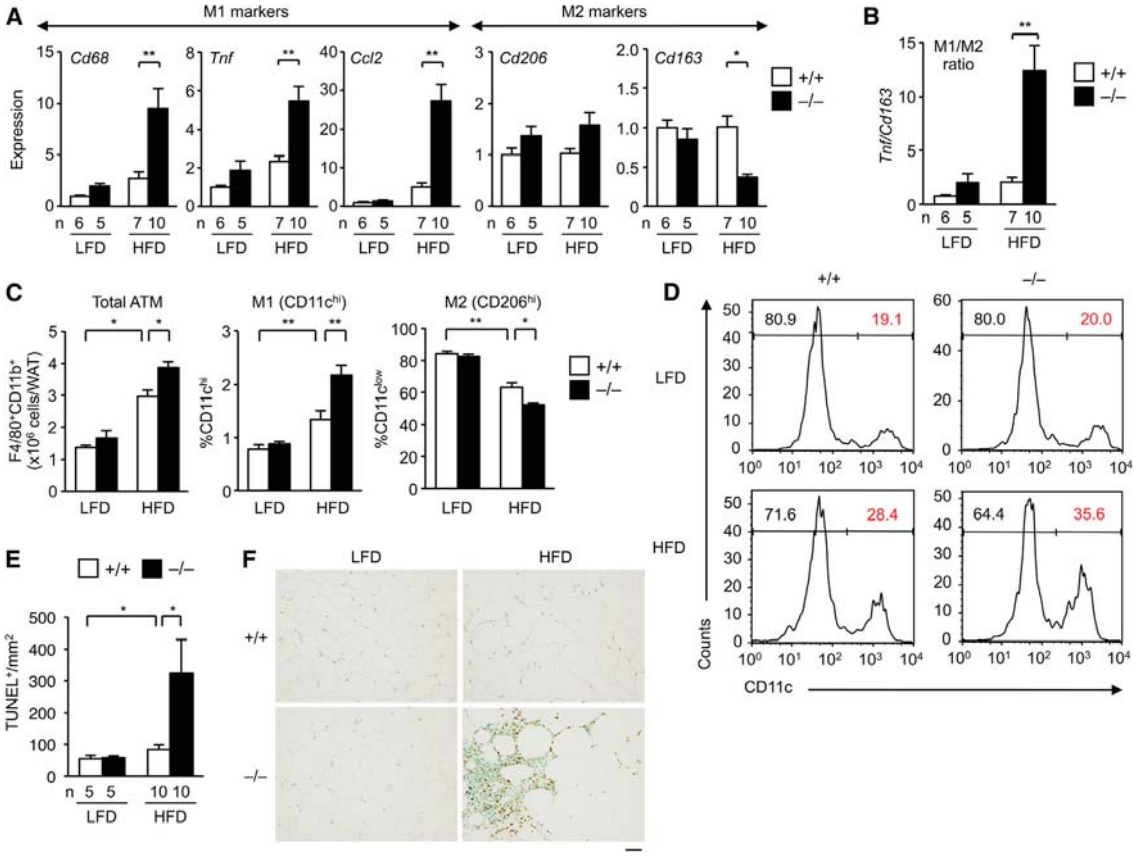

Figure 4. Exacerbated Adipose Tissue Inflammation in HFD-Fed *Pla2g5*$^{-/-}$ Mice

(A) Expression of M1 or M2 macrophage markers normalized by *Gapdh* in WAT of *Pla2g5*$^{+/+}$ and *Pla2g5*$^{-/-}$ mice, with their expression in *Pla2g5*$^{+/+}$ mice on a LFD being regarded as 1.

(B) Ratios of M1 (*Tnf*) to M2 (*Cd163*) genes.

(C) FACS analysis of adipose tissue macrophages (ATM) from *Pla2g5*$^{+/+}$ and *Pla2g5*$^{-/-}$ mice. Counts of F4/80$^+$CD11b$^+$ ATM and proportions of CD11c^{hi} (M1) and CD206^{hi} (M2) macrophages in SVF from WAT (n = 4).

(D) Representative FACS profiles of CD11c$^+$ cells in the SVF.

(E and F) TUNEL staining of WAT in *Pla2g5*$^{+/+}$ and *Pla2g5*$^{-/-}$ mice. Average scores of TUNEL-positive cells (E) and representative images (scale bar, 50 μm) (F).

Mice were fed a LFD or HFD for 26 weeks. Data are compiled from (A, B, and E) or representative of (C, D, and F) two experiments. Mean ± SEM; *$p < 0.05$, **$p < 0.01$.

PUFAs mobilized by PLA2G5 from LDL, may allow the polarization from M1 to M2 macrophages by attenuating the PA-induced stress response, which underscores a mechanistic link between PLA2G5-driven LDL hydrolysis and anti-inflammation in WAT.

PLA2G5 Is a Th2/M2-Prone sPLA$_2$

While T helper 2 (Th2) cytokines are proallergic, they facilitate M2 macrophage polarization, thereby counteracting adipose tissue inflammation and insulin resistance (Odegaard and Chawla, 2013). It has been shown that PLA2G5 from both hematopoietic and nonhematopoietic origins regulates the Th2 response and thereby asthma (Giannattasio et al., 2010; Henderson et al., 2013). Indeed, when WT mice were immunized intraperitoneally with ovalbumin (OVA), lymph node cells from *Pla2g5*$^{-/-}$ mice expressed levels of IL-4 and IL-13 lower than those from *Pla2g5*$^{+/+}$ mice upon OVA challenge ex vivo (Figure S5G). Serum levels of total or OVA-specific immunoglobulin E (IgE) were lower in *Pla2g5*$^{-/-}$ mice than in *Pla2g5*$^{+/+}$ mice (Figure S5H). Moreover, beyond the crucial role of adipocyte- rather than macrophage-derived PLA2G5 in obesity, *Pla2g5* expression in BMDMs was markedly induced by M2-skewing Th2 cytokines (IL-4 and IL-13) and was unaffected or reduced by M1-skewing TLR agonists (LPS and zymozan) or Th1 cytokines (IFN-γ and granulocyte-macrophage colony-stimulating factor [GM-CSF]) among others (Figures S5I and S5J). In ex vivo skewing culture of splenic naive CD4$^+$ T cells, *Pla2g5* was induced preferentially in IL-4-driven Th2 cells (Figure S5K). In the context of obesity, the WAT expression of *Il33*, a stromal Th2 cytokine that increases M2 macrophages and suppresses adipose tissue inflammation (Miller et al., 2010), was lower in HFD-fed *Pla2g5*$^{-/-}$ mice than in replicate *Pla2g5*$^{+/+}$ mice (Figure 5I). Thus, PLA2G5 is a unique sPLA$_2$ that is induced by Th2 cytokines and facilitates the Th2 and M2 responses. *Pla2g5*$^{-/-}$ mice are Th2/M2 insufficient, and this intrinsic immune balance shift may also underlie the exacerbated adipose tissue inflammation.

Reduced Adiposity in Adipocyte-Specific *Pla2g5* Transgenic Mice

To explore whether the forced overexpression of PLA2G5 in the WAT would yield outcomes opposite to its deletion, we

Please cite this article in press as: Sato et al., The Adipocyte-Inducible Secreted Phospholipases PLA2G5 and PLA2G2E Play Distinct Roles in Obesity, Cell Metabolism (2014), http://dx.doi.org/10.1016/j.cmet.2014.05.002

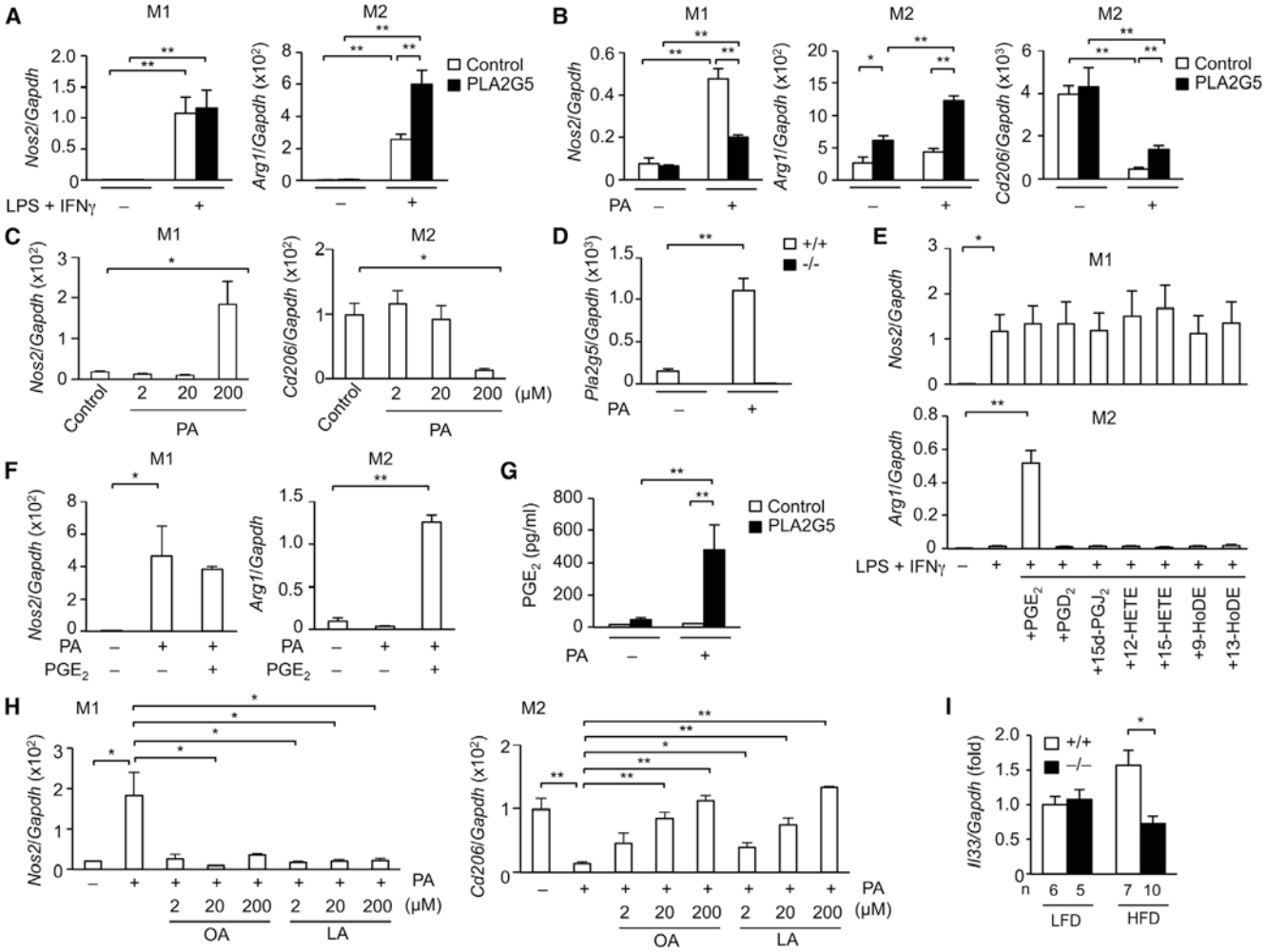

Figure 5. PLA2G5 Promotes M2 Macrophage Polarization

(A and B) Expression of M1 and M2 macrophage markers in WT BMDMs cultured for 24 hr with (+) or without (−) LPS+IFN-γ (A) or 200 μM PA (B) in the presence or absence of 70 nM PLA2G5 (n = 7).

(C) Expression of M1 and M2 macrophage markers in WT BMDMs after culture for 24 hr with various concentrations of PA (n = 6).

(D) Expression of *Pla2g5* in *Pla2g5*$^{+/+}$ and *Pla2g5*$^{-/-}$ BMDMs after culture for 24 hr with 200 μM PA (n = 6).

(E and F) Expression of M1 and M2 markers in WT BMDMs cultured for 24 hr with (+) or without (−) LPS+IFN-γ (D) or 200 μM PA (E) in the presence or absence of 1 μM lipid mediators (n = 6).

(G) PGE_2 generation by WT BMDMs treated for 6 hr with PLA2G5 in the presence (+) or absence (−) of 200 μM PA (n = 3).

(H) Effects of OA or LA on the expression of M1 or M2 macrophage markers in WT BMDMs treated for 24 hr with 200 μM PA (n = 3).

(I) Expression of *Il33* relative to *Gapdh* in WAT of *Pla2g5*$^{+/+}$ and *Pla2g5*$^{-/-}$ mice fed a LFD or HFD for 26 weeks.

Data are compiled from (A–F and I) or representative of (G and H) two experiments. Mean ± SEM; *p < 0.05, **p < 0.01.

generated adipocyte-specific *Pla2g5* transgenic mice (*Fabp4-Pla2g5*$^{tg/+}$) by mating *LNL-Pla2g5*$^{tg/+}$ mice (Ohtsuki et al., 2006), in which the *Pla2g5* transgene was silent, with *Fabp4-Cre*$^{tg/+}$ mice, in which Cre recombinase is expressed under control of the adipocyte-specific *Fabp4* promoter (Figure S6A). *Fabp4-Pla2g5*$^{tg/+}$ mice were born normally and grew to adulthood. As expected, expression of *Pla2g5* was robustly increased in perigonadal WAT, but not in other tissues, in *Fabp4-Pla2g5*$^{tg/+}$ mice compared to control *LNL-Pla2g5*$^{tg/+}$ mice (Figure S6B). Even on a LFD, where the influence of diet-inducible endogenous PLA2G5 is negligible, *Fabp4-Pla2g5*$^{tg/+}$ mice had body weight significantly lower than that of age-matched control mice (Figure S6C). CT scanning revealed a reduced adiposity in *Fabp4-Pla2g5*$^{tg/+}$ mice relative to control mice (Figure S6D). Phospholipid levels in plasma and LDL were significantly lower in *Fabp4-Pla2g5*$^{tg/+}$ mice than in control mice (Figure S6E). Moreover, WAT expression levels of proinflammatory genes, but not lipogenic genes, tended to be lower in *Pla2g5*$^{tg/+}$ mice than in control mice (Figure S6F). After 6 weeks of HFD feeding, when the induction of endogenous *Pla2g5* was still minimal (Figure S1B), *Fabp4-Pla2g5*$^{tg/+}$ mice displayed better insulin sensitivity and lower WAT expression of *Ccl2* compared to control mice (Figures S6G and S6H). Collectively, the data for adipocyte-specific PLA2G5 overexpression reciprocated those for PLA2G5 deficiency.

Please cite this article in press as: Sato et al., The Adipocyte-Inducible Secreted Phospholipases PLA2G5 and PLA2G2E Play Distinct Roles in Obesity, Cell Metabolism (2014), http://dx.doi.org/10.1016/j.cmet.2014.05.002

Reduced Adiposity and Altered Lipoprotein Profiles in *Pla2g2e*$^{-/-}$ Mice

To address the roles of PLA2G2E, we generated *Pla2g2e*$^{-/-}$ mice (Figures S7A and S7B). Expression of mRNA and protein for PLA2G2E was absent in WAT of HFD-fed *Pla2g2e*$^{-/-}$ mice (Figure S7C). On a HFD, obesity and weight gain tended to be lower (though statistically insignificant) in *Pla2g2e*$^{-/-}$ mice than in *Pla2g2e*$^{+/+}$ mice (Figures 6A and 6B). Volumes of total, visceral, and subcutaneous fats (Figure 6C) and adipocyte size in perigonadal WAT (Figure 6D) were significantly reduced in HFD-fed *Pla2g2e*$^{-/-}$ mice relative to *Pla2g2e*$^{+/+}$ mice. Plasma leptin and insulin levels (Figures S7D and S7E), glucose and insulin tolerances (Figures S7F and S7G), food intake, locomotion and oxygen consumption (Figures S7H–S7J), and WAT expression of adipogenenic, lipogenic, lipolytic, and inflammatory genes (Figure S7K) did not differ between HFD-fed *Pla2g2e*$^{+/+}$ and *Pla2g2e*$^{-/-}$ mice. HFD-induced fatty liver was mildly ameliorated by PLA2G2E deficiency, as revealed by reductions of hepatic lipid deposition (Figures 6E and 6F), plasma ALT, and aspartate amino transferase (AST) levels (Figure 6G), and hepatic expression of some genes for lipid storage and inflammation (Figure S7L) in HFD-fed *Pla2g2e*$^{-/-}$ mice compared to WT littermates. Lower hepatic *Lpl* expression in *Pla2g2e*$^{-/-}$ mice (Figure S7L) might partly contribute to the reduced fat uptake into the liver.

HFD-induced increases in plasma phospholipids and cholesterol were lower in *Pla2g2e*$^{-/-}$ mice than in *Pla2g2e*$^{+/+}$ mice (Figure 6H), suggesting that PLA2G2E alters lipoprotein composition. Indeed, phospholipids, TG, and cholesterol in VLDL, LDL, and HDL were significantly lower in HFD-fed *Pla2g2e*$^{-/-}$ mice than in *Pla2g2e*$^{+/+}$ mice (Figures 6I and S7M). ESI-MS revealed that LDL (Figure 6J) and HDL (data not shown) in *Pla2g2e*$^{-/-}$ mice contained more PE and PS species, with no apparent fatty acid selectivity, than those in *Pla2g2e*$^{+/+}$ mice, while PC species did not differ in both genotypes, suggesting that adipocyte-derived PLA2G2E acts on PE and PS in favor of PC in lipoproteins. The increase of these minor phospholipids by PLA2G2E deficiency may eventually decrease the relative proportion of PC and other lipids in lipoproteins, thereby affecting lipid partitioning among tissues.

Taken together, PLA2G5 is protective against metabolic disorders by hydrolyzing PC in hyperlipidemic LDL to release unsaturated fatty acids, which attenuate adipose tissue inflammation through M2 macrophage skewing, while PLA2G2E mildly promotes adiposity and fatty liver by altering the proportion of PE and PS in lipoproteins (Figure 7).

DISCUSSION

Adipocyte hypertrophy results in secretion of bioactive factors such as adipokines, chemokines, and free fatty acids, which adversely affect inflammation and tissue remodeling while providing valuable protection against lipotoxic effects of excess lipid exposure (Després and Lemieux, 2006). We now show that two particular $sPLA_2$s are induced in hypertrophic adipocytes and play distinct roles in metabolic control in the context of diet-induced obesity. Our results add the $sPLA_2$ family to a growing list of extracellular lipolytic enzymes that can control systemic metabolic states and give another insight into the paracrine role of $sPLA_2$ in response to a given microenvironmental cue.

The obesity-driven induction of PLA2G5 in hypertrophic adipocytes, along with its constitutive expression at relatively high levels in the heart and skeletal muscle, which have a high demand for lipid as an energy source, suggests that one of the primary roles of this $sPLA_2$ may be related to the regulation of energy metabolism. We show here that *Pla2g5* ablation exacerbates diet-induced obesity, hyperlilidemia, and insulin resistance, providing insight into the beneficial role of PLA2G5 in metabolic disorders. PLA2G5 can hydrolyze PC in lipoproteins in vitro (Sato et al., 2008), and our present results show that this reaction does occur in vivo in the context of obesity, where adipocyte-driven PLA2G5 hydrolyzes excess PC in lipid-overladen LDL, eventually protecting from hyperlipidemia. In this regard, the metabolic effects of PLA2G5 are similar to those of lipoprotein lipase, whose expression also shows a reciprocal relationship with obesity-related traits (Chen et al., 2008). Even though it has been thought that mice are not always good models to study LDL metabolism, as they use VLDL and HDL primarily, our results show that LDL metabolism by $sPLA_2$ can influence systemic metabolic states. The increased LDL-TG levels and the reduced physical activities in *Pla2g5*$^{-/-}$ mice could impact adipocyte hypertrophy, hepatic steatosis, and WAT inflammation. Importantly, *PLA2G5* expression in human WAT inversely correlates with plasma LDL levels, implying a human relevance of our observations. Moreover, our findings are also compatible with the association of *PLA2G5* mutations with LDL levels in subjects with type 2 diabetes or obesity (Sergouniotis et al., 2011; Wootton et al., 2007).

Importantly, PLA2G5 plays an anti-inflammatory role in obesity, which likely makes a major contribution to the exacerbated obesity, insulin resistance, and hyperlipidemia in *Pla2g5*$^{-/-}$ mice. This action of PLA2G5 depends on its capacity to hydrolyze phospholipids in LDL to release unsaturated fatty acids, which can allow the polarization shift of macrophages from the M1 to M2 state. Reportedly, fatty acids released from lipoproteins by venom $sPLA_2$ or lipoprotein lipase can facilitate anti-inflammatory responses in vitro (Ahmed et al., 2006; Duncan et al., 2010; Namgaladze et al., 2010). Herein, we demonstrate that unsaturated fatty acids including OA > LA, which are supplied by PLA2G5-driven hydrolysis of PC in hyperlipidemic LDL, prevent PA-induced M1 macrophage polarization, likely through attenuating the ER stress, revealing a functional link between lipoprotein metabolism and anti-inflammation by this $sPLA_2$. This mechanism fits with the view that PLA2G5 displays an apparent (even if not strict) substrate preference for PC bearing a fatty acid with a low degree of unsaturation. Our study provides in vivo evidence that $sPLA_2$ acts in this manner, thus providing a rationale for the long-standing question on the physiological importance of lipoprotein hydrolysis by this enzyme family and revealing an anti-inflammatory mechanism exerted by a particular $sPLA_2$. Nonetheless, it cannot be fully ruled out that the mobilization of PGE_2, a ω6 AA-derived eicosanoid that promotes M2 macrophage skewing (Heusinkveld et al., 2011), or ω3 PUFA metabolites, which are protective against metabolic disorders (Oh and Olefsky, 2012; Spite et al., 2014), might also partly underlie the antiobese action of PLA2G5.

As another intriguing feature of PLA2G5, we show that it is a "Th2/M2-prone $sPLA_2$" that allows the immune balance shift toward the Th2/M2 status. Given the increased metabolic

Please cite this article in press as: Sato et al., The Adipocyte-Inducible Secreted Phospholipases PLA2G5 and PLA2G2E Play Distinct Roles in Obesity, Cell Metabolism (2014), http://dx.doi.org/10.1016/j.cmet.2014.05.002

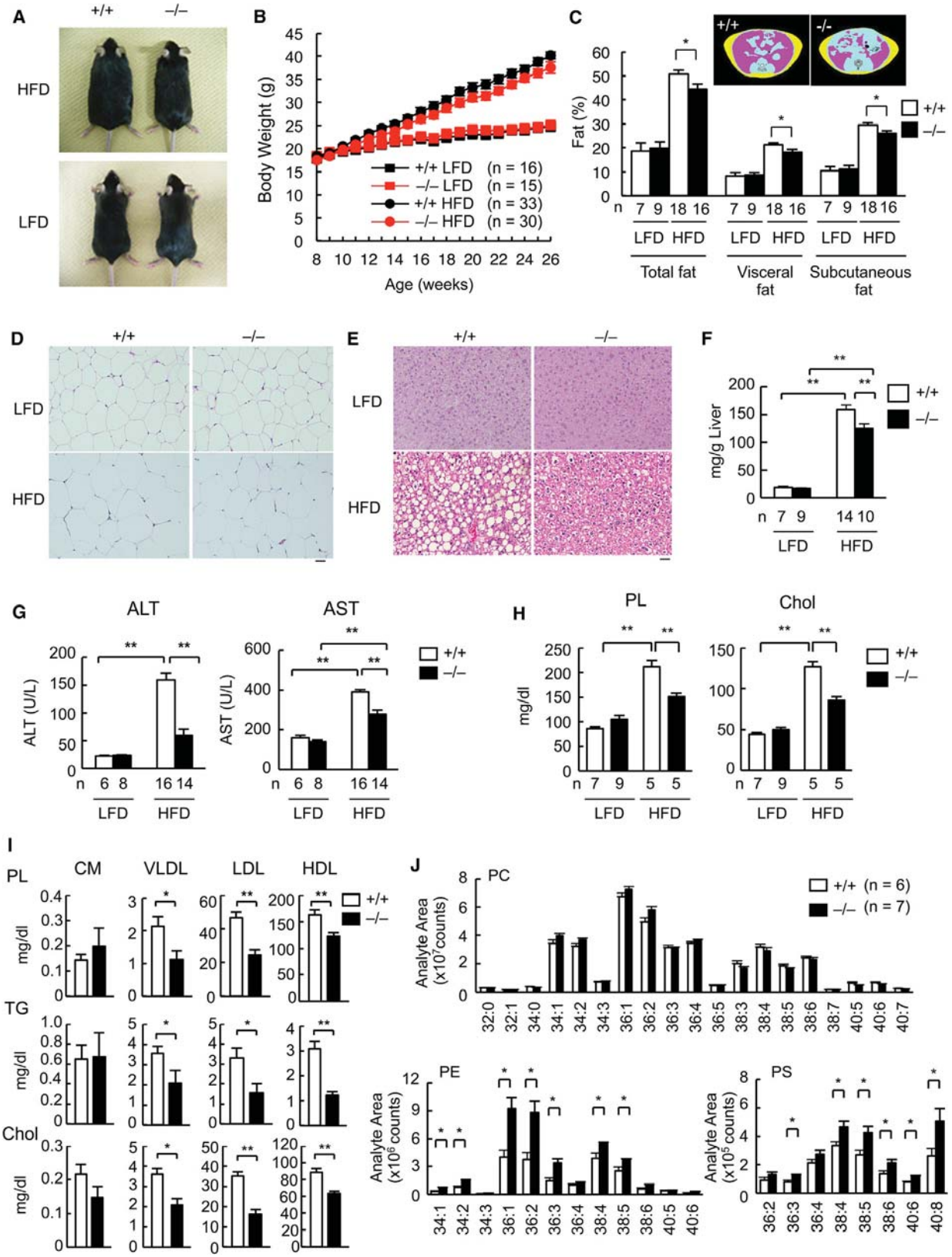

Figure 6. Altered Diet-Induced Adiposity, Fatty Liver, and Lipoproteins in *Pla2g2e*$^{-/-}$ Mice

(A) Representative photos of *Pla2g2e*$^{+/+}$ and *Pla2g2e*$^{-/-}$ mice fed a LFD or HFD.

(B) Body weights of *Pla2g2e*$^{+/+}$ and *Pla2g2e*$^{-/-}$ mice fed a LFD or HFD for the indicated periods.

(legend continued on next page)

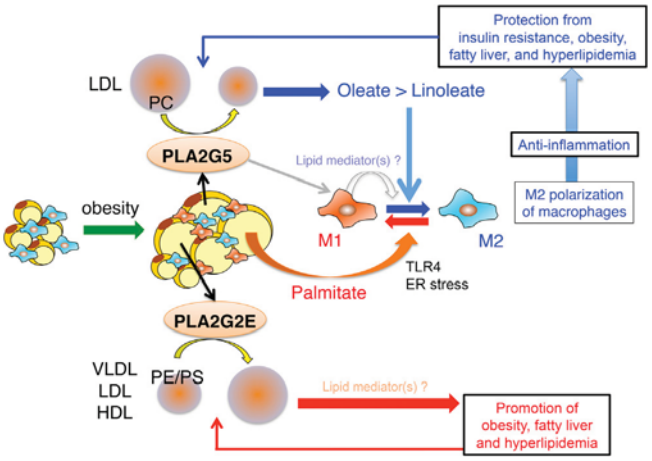

Figure 7. Schematic Diagram of the Roles of Metabolic sPLA$_2$s

In obesity, PLA2G2E is induced in adipocytes in accordance with adipogenesis and hydrolyzes PE and PS in VLDL, LDL, and HDL, eventually promoting fat storage in WAT and liver. Subsequently, obesity-associated stress induces PLA2G5 in hypertrophic adipocytes. PLA2G5 hydrolyzes PC in hyperlipidemic LDL and facilitates the skewing of macrophages from M1 to M2 subsets, thereby playing protective roles against adipose tissue inflammation, insulin resistance, obesity, fatty liver, and hyperlipidemia. Saturated fatty acids (e.g., palmitate) supplied abundantly from adipocytes trigger M1 polarization of macrophages, which is ameliorated by PLA2G5-driven unsaturated fatty acids (oleate > linoleate) from LDL or possibly some lipid mediators from macrophages. It remains unknown whether particular PLA2G2E-produced lipid mediator(s) would participate in this process.

disorders by genetic deletion of Th2 or M2 inducers (e.g., *Il4*, *Il13*, *Il33*, *Stat6*, or *Pparg*) (Odegaard and Chawla, 2013), the lack of PLA2G5 may also decrease the whole-body Th2-M2 status, thereby aggravating obesity-related inflammation. This notion agrees with the fact that *Pla2g5*$^{-/-}$ mice are resistant to asthma (Giannattasio et al., 2010; Henderson et al., 2013), where Th2 cells and M2 macrophages promote allergy, while they suffer from exaggerated arthritis or infection (Balestrieri et al., 2009; Boilard et al., 2010), where Th2 immunity counteracts Th1/Th17-based inflammation, thus accounting for the pro- versus anti-inflammatory actions of PLA2G5 in distinct immunopathological settings. As the phagocytotic activities are distinct among macrophage subsets (Leidi et al., 2009; Titos et al., 2011), the altered M1/M2 ratio of macrophages in obese *Pla2g5*$^{-/-}$ WAT could explain the perturbed clearance of dead cells. This idea also accords with the finding that *Pla2g5* ablation decreases macrophage uptake of exogenous materials (Balestrieri et al., 2009; Boilard et al., 2010).

We also show the in vivo role of PLA2G2E as another obesity-induced, adipocyte-derived sPLA$_2$. In contrast to PLA2G5 that hydrolyzes PC in LDL, PLA2G2E acts on PE and PS in VLDL, LDL, and HDL. As such, PLA2G2E alters lipid composition in lipoprotein particles, eventually moderately facilitating fat deposition in tissues. Although little is known about the role of PE or PS in lipoproteins, our study has shed light on the importance of these minor lipoprotein phospholipids in the metabolic regulation and opened an opportunity to analyze this issue using *Pla2g2e*$^{-/-}$ mice as a tool. As the increase of negative charges in lipoproteins by oxidative modification renders the particles smaller (Hidaka et al., 2005), the increase of anionic phospholipids (e.g., PS) in lipoproteins may afford a similar effect. Lipoproteins with increased negative charges are more susceptible to hydrolysis by hepatic lipase, resulting in smaller particles (Boucher et al., 2007). Anionic phospholipids decrease the affinity of ApoE for its receptor, thereby reducing lipid transfer into tissues (Yamamoto and Ryan, 2007). Alternatively, Lyso-PE or Lyso-PS produced by PLA2G2E might have some metabolic effects, a possibility that needs to be addressed. Compatible with our present study, PLA2G2A in place of PLA2G2E is induced in obese rats in which the metabolic symptoms are blocked by a PLA2G2A inhibitor (Iyer et al., 2012).

In summary, our study underscores the physiological relevance of lipoprotein hydrolysis by sPLA$_2$s, highlights metabolic sPLA$_2$s as integrated regulators of immune and metabolic responses, and brings about a shift toward a better understanding of the biological roles of this extracellular lipolytic enzyme family as a metabolic coordinator. The contrasting metabolic effects of PLA2G5 and PLA2G2E are reminiscent of distinct roles of PLA2G5 and PLA2G2A in arthritis (Boilard et al., 2010), PLA2G5 and PLA2G10 in atherosclerosis (Ait-Oufella et al., 2013; Bostrom et al., 2007), or PLA2G2D and PLA2G5 in antigen-presenting cells (Giannattasio et al., 2010; Miki et al., 2013), warning about the use of pan-sPLA$_2$ inhibitors for therapy and pointing to an alternative strategy to use a sPLA$_2$ inhibitor specific for individual sPLA$_2$s. Targeting the metabolic sPLA$_2$s and their organ expression will be a challenge, since these enzymes appear to play highly selective roles in specific organs and disease states.

EXPERIMENTAL PROCEDURES

Mice

Pla2g5$^{-/-}$ (Satake et al., 2004), *Pla2g5*$^{tg/+}$ (Ohtsuki et al., 2006), and their littermate control mice were backcrossed onto the C57BL/6 mice (Japan SLC) for >12 generations. Generation of *Pla2g2e*$^{-/-}$ mice is detailed in Supplemental Information. *Lep*$^{ob/ob}$ mice and *Fabp4-Cre* transgenic mice were obtained from Jackson Laboratory. All mice were housed in climate-controlled (23°C) pathogen-free facilities with a 12 hr light-dark cycle, with free access to standard LFD (CE2; CLEA Japan) and water. Knockout and littermate WT mice (8-week-old female) were placed on a HFD (High fat diet 32; CLEA Japan)

(C) CT analysis of fat volumes in *Pla2g2e*$^{+/+}$ and *Pla2g2e*$^{-/-}$ mice. Pink and yellow areas indicate visceral and subcutaneous fats in HFD-fed mice, respectively (inset).

(D and E) Hematoxylin and eosin staining of WAT (D) or liver (E) from *Pla2g2e*$^{+/+}$ and *Pla2g2e*$^{-/-}$ mice (scale bar, 50 μm).

(F and G) Levels of hepatic TG (F) and plasma ALT and AST (G) in *Pla2g2e*$^{+/+}$ and *Pla2g2e*$^{-/-}$ mice.

(H) Plasma levels of phospholipids (PL) and cholesterol (Chol) in *Pla2g2e*$^{+/+}$ and *Pla2g2e*$^{-/-}$ mice.

(I) PL, TG, and Chol levels in lipoproteins from HFD-fed *Pla2g2e*$^{+/+}$ and *Pla2g2e*$^{-/-}$ mice (n = 5).

(J) ESI-MS of PC, PE, and PS in LDL from HFD-fed *Pla2g2e*$^{+/+}$ and *Pla2g2e*$^{-/-}$ mice.

Mice were fed a LFD or HFD for 16 (A and C) or 18 (D–J) weeks. Data are compiled from two (H–J) or three (B, C, F, and G) experiments. Representative images of two experiments are shown (A, D, and E). Mean ± SEM; *$p < 0.05$, **$p < 0.01$.

or LFD for appropriate periods. All procedures were performed in accordance with approvals by the Institutional Animal Care and Use Committees of Tokyo Metropolitan Institute of Medical Science, Showa University, and the University of Washington.

Quantitative RT-PCR

Total RNA was extracted from tissues using TRIzol reagent (Invitrogen). First-strand cDNA synthesis was performed using a High Capacity cDNA Reverse Transcriptase Kit (Applied Biosystems). PCR reactions were carried out using a Power SYBR Green PCR system (Applied Biosystems) or a TaqMan Gene Expression System (Applied Biosystems) on the ABI7300 Real Time PCR system (Applied Biosystems). The probe/primer sets used are listed in Tables S3 and S4.

Microarray

Total RNA was extracted from WAT derived from female C57BL/6 mice fed a LFD or HFD for 18 weeks and purified using the RNeasy Mini Kit (QIAGEN). The quality of RNA was assessed with a 2100 Bioanalyzer (Agilent Technologies). Both cDNA and cRNA were synthesized with a Low Input QuickAmp Labeling Kit according to the manufacturer's protocol (Agilent Technologies). Samples were hybridized to the Whole Mouse Genome Microarray Kit (4 × 44K; Agilent Technologies), washed, and then scanned using a SureScan Microarray Scanner (Agilent Technologies). Microarray data were analyzed with Feature Extraction software (Agilent Technologies) and then imported into GeneSpring GX software (Agilent Technologies). Probes were normalized by quantile normalization among all microarray data.

Flow Cytometry

The isolated SVF cells were incubated with either labeled monoclonal antibody or isotype control antibody (hamster IgG [HTK888], rat IgG$_{2a}$ [RTK2758], or rat IgG$_{2b}$ [RTK4530]; BioLegend) and analyzed by flow cytometry with a FACSAria III (BD Biosciences) and FlowJo (Tree Star) software. The antibodies used were specific for mouse F4/80 (BM8; BioLegend), CD11b (M1/70; BioLegend), CD11c (N418; eBioscience), and CD206 (C068C2; BioLegend).

Glucose and Insulin Tolerance Tests

Mice were fasted for 16 and 6 hr before intraperitoneal injection of glucose (2 mg glucose/g body weight) (Wako) and insulin (0.75 mIU/g body weight) (Eli Lilly) in saline, respectively. Blood glucose concentrations were monitored at various time intervals using a Medisafe-Mini blood glucose monitoring system (Terumo).

Measurement of Serum Biomedical Markers

Serum insulin and leptin levels were quantified by a mouse insulin ELISA kit (Mercodia) and a leptin immunoassay kit (R&D Systems), respectively. Serum ALT and AST levels were quantified using the transaminase CII-test Wako kit (Wako).

CT Analysis

Mice were anesthetized with nembutal (0.5 mg/g body weight) (Dainippon Sumitomo Pharma), and their adiposity was analyzed using the micro-CT systems eXplore Lucus Micro CT Scanner (GE Healthcare) or Latheta LCT-100 (Aloka).

Oxygen Consumption and Locomotor Activity

Oxygen consumption was measured every 3 min over 24 hr under resting conditions using an MK-5000RQ metabolism measuring system for small animals (Muromachi Kikai). For measurement of basal locomotor activity, mice were placed into chambers of an ACTIMO-S food intake, drinking, and locomotor activity monitoring system (Shintechno). Food and water were provided ad libitum. Mice were allowed to acclimatize in the chambers for 24 hr, and then their physical activities were measured over the next 24 hr.

Analyses of Plasma Lipids and Lipoproteins

Analysis of plasma lipoproteins was performed by LipoSearch (Skylight Biotech). Plasma cholesterol, phospholipid, LPC, TG, and NEFA levels were determined with a Determinar TC2 (Kyowa Medex), a Phospholipid C Test (Wako), a LPC Assay kit (AZWELL), a Determinar TG2 (Kyowa Medex), and a NEFA C Kit (Wako), respectively.

ESI-MS/MS

Lipid analysis was performed using a 4000 QTRAP quadrupole-linear ion trap hybrid MS (AB SCIEX) with liquid chromatography (LC-20AP; Shimazu) combined with a HTS PAL autosampler (CTC Analytics AG), as detailed in Supplemental Information.

Cell Culture Studies

Studies using adipocytes and immune cells are detailed in Supplemental Information.

Human Samples

Mesenteric WAT and fatty appendices were obtained by curative resection from 64 patients with colorectal tumors, all of whom underwent elective surgical colorectomy at the Kumamoto University Hospital (Kumamoto, Japan) from March 1, 2012 to August 31, 2013. The clinical characteristics are summarized in Table S2. The study was approved by the Ethics Committees of Kumamoto University, with written informed consent from all patients.

Statistical Analyses

All values are given as the mean ± SEM. Differences between two groups were assessed by using the unpaired two-tailed t test. Data involving more than two groups were assessed by ANOVA, and relationships between clinical and metabolic parameters were assessed by Spearman's rank correlation test. Correlation coefficients (R) and probability (P) values were calculated with the Excel Statistical Program File yStat 2008 (Igaku Tosho Shuppan).

ACCESSION NUMBERS

The GEO accession number for microarray data reported in this paper is GSE56038.

SUPPLEMENTAL INFORMATION

Supplemental Information includes Supplemental Experimental Procedures, seven figures, and four tables and can be found with this article online at http://dx.doi.org/10.1016/j.cmet.2014.05.002.

ACKNOWLEDGMENTS

We thank Dr. Jonathan P. Arm (Novartis Pharma) for providing us *Pla2g5*$^{-/-}$ mice and Dr. Osamu Kaminuma (Tokyo Metroplitan Insutitute of Medical Science) for providing us mRNAs from naive and polarized T cells. This work was supported by grants-in-aid for Scientific Research from the Ministry of Education, Culture, Sports, Science and Technology of Japan (22116005 and 24390021 to M.M.; 23790120 and 25860059 to H.S.; 24117724 and 23790119 to Y.T.), CREST from the Japan Science and Technology Agency (to M.M.), the Uehara, Mitsubishi, Terumo and Toray Science Foundations (to M.M.), and grant HL36235 (to M.H.G.) from the National Institutes of Health.

Received: August 23, 2013
Revised: February 19, 2014
Accepted: April 2, 2014
Published: June 5, 2014

REFERENCES

Ahmed, W., Orasanu, G., Nehra, V., Asatryan, L., Rader, D.J., Ziouzenkova, O., and Plutzky, J. (2006). High-density lipoprotein hydrolysis by endothelial lipase activates PPARalpha: a candidate mechanism for high-density lipoprotein-mediated repression of leukocyte adhesion. Circ. Res. *98*, 490–498.

Ait-Oufella, H., Herbin, O., Lahoute, C., Coatrieux, C., Loyer, X., Joffre, J., Laurans, L., Ramkhelawon, B., Blanc-Brude, O., Karabina, S., et al. (2013). Group X secreted phospholipase A$_2$ limits the development of atherosclerosis in LDL receptor-null mice. Arterioscler. Thromb. Vasc. Biol. *33*, 466–473.

Balestrieri, B., Maekawa, A., Xing, W., Gelb, M.H., Katz, H.R., and Arm, J.P. (2009). Group V secretory phospholipase A$_2$ modulates phagosome maturation

and regulates the innate immune response against *Candida albicans*. J. Immunol. *182*, 4891–4898.

Boilard, E., Lai, Y., Larabee, K., Balestrieri, B., Ghomashchi, F., Fujioka, D., Gobezie, R., Coblyn, J.S., Weinblatt, M.E., Massarotti, E.M., et al. (2010). A novel anti-inflammatory role for secretory phospholipase A_2 in immune complex-mediated arthritis. EMBO Mol Med *2*, 172–187.

Bostrom, M.A., Boyanovsky, B.B., Jordan, C.T., Wadsworth, M.P., Taatjes, D.J., de Beer, F.C., and Webb, N.R. (2007). Group v secretory phospholipase A_2 promotes atherosclerosis: evidence from genetically altered mice. Arterioscler. Thromb. Vasc. Biol. *27*, 600–606.

Boucher, J.G., Nguyen, T., and Sparks, D.L. (2007). Lipoprotein electrostatic properties regulate hepatic lipase association and activity. Biochem. Cell Biol. *85*, 696–708.

Chen, Y., Zhu, J., Lum, P.Y., Yang, X., Pinto, S., MacNeil, D.J., Zhang, C., Lamb, J., Edwards, S., Sieberts, S.K., et al. (2008). Variations in DNA elucidate molecular networks that cause disease. Nature *452*, 429–435.

Chiu, H.K., Qian, K., Ogimoto, K., Morton, G.J., Wisse, B.E., Agrawal, N., McDonald, T.O., Schwartz, M.W., and Dichek, H.L. (2010). Mice lacking hepatic lipase are lean and protected against diet-induced obesity and hepatic steatosis. Endocrinology *151*, 993–1001.

Cinti, S., Mitchell, G., Barbatelli, G., Murano, I., Ceresi, E., Faloia, E., Wang, S., Fortier, M., Greenberg, A.S., and Obin, M.S. (2005). Adipocyte death defines macrophage localization and function in adipose tissue of obese mice and humans. J. Lipid Res. *46*, 2347–2355.

Després, J.P., and Lemieux, I. (2006). Abdominal obesity and metabolic syndrome. Nature *444*, 881–887.

Duncan, J.G., Bharadwaj, K.G., Fong, J.L., Mitra, R., Sambandam, N., Courtois, M.R., Lavine, K.J., Goldberg, I.J., and Kelly, D.P. (2010). Rescue of cardiomyopathy in peroxisome proliferator-activated receptor-α transgenic mice by deletion of lipoprotein lipase identifies sources of cardiac lipids and peroxisome proliferator-activated receptor-α activators. Circulation *121*, 426–435.

Giannattasio, G., Fujioka, D., Xing, W., Katz, H.R., Boyce, J.A., and Balestrieri, B. (2010). Group V secretory phospholipase A_2 reveals its role in house dust mite-induced allergic pulmonary inflammation by regulation of dendritic cell function. J. Immunol. *185*, 4430–4438.

Haemmerle, G., Lass, A., Zimmermann, R., Gorkiewicz, G., Meyer, C., Rozman, J., Heldmaier, G., Maier, R., Theussl, C., Eder, S., et al. (2006). Defective lipolysis and altered energy metabolism in mice lacking adipose triglyceride lipase. Science *312*, 734–737.

Henderson, W.R., Jr., Ye, X., Lai, Y., Ni, Z., Bollinger, J.G., Tien, Y.T., Chi, E.Y., and Gelb, M.H. (2013). Key role of group v secreted phospholipase A_2 in Th2 cytokine and dendritic cell-driven airway hyperresponsiveness and remodeling. PLoS ONE *8*, e56172.

Heusinkveld, M., de Vos van Steenwijk, P.J., Goedemans, R., Ramwadhdoebe, T.H., Gorter, A., Welters, M.J., van Hall, T., and van der Burg, S.H. (2011). M2 macrophages induced by prostaglandin E_2 and IL-6 from cervical carcinoma are switched to activated M1 macrophages by $CD4^+$ Th1 cells. J. Immunol. *187*, 1157–1165.

Hidaka, A., Inoue, K., Kutsukake, S., Adachi, M., Kakuta, Y., and Kojo, S. (2005). Decrease in the particle size of low-density lipoprotein (LDL) by oxidation. Bioorg. Med. Chem. Lett. *15*, 2781–2785.

Hotamisligil, G.S. (2006). Inflammation and metabolic disorders. Nature *444*, 860–867.

Ivandic, B., Castellani, L.W., Wang, X.P., Qiao, J.H., Mehrabian, M., Navab, M., Fogelman, A.M., Grass, D.S., Swanson, M.E., de Beer, M.C., et al. (1999). Role of group II secretory phospholipase A_2 in atherosclerosis: 1. Increased atherogenesis and altered lipoproteins in transgenic mice expressing group IIa phospholipase A_2. Arterioscler. Thromb. Vasc. Biol. *19*, 1284–1290.

Iyer, A., Lim, J., Poudyal, H., Reid, R.C., Suen, J.Y., Webster, J., Prins, J.B., Whitehead, J.P., Fairlie, D.P., and Brown, L. (2012). An inhibitor of phospholipase A_2 group IIA modulates adipocyte signaling and protects against diet-induced metabolic syndrome in rats. Diabetes *61*, 2320–2329.

Jaworski, K., Ahmadian, M., Duncan, R.E., Sarkadi-Nagy, E., Varady, K.A., Hellerstein, M.K., Lee, H.Y., Samuel, V.T., Shulman, G.I., Kim, K.H., et al. (2009). AdPLA ablation increases lipolysis and prevents obesity induced by high-fat feeding or leptin deficiency. Nat. Med. *15*, 159–168.

Leidi, M., Gotti, E., Bologna, L., Miranda, E., Rimoldi, M., Sica, A., Roncalli, M., Palumbo, G.A., Introna, M., and Golay, J. (2009). M2 macrophages phagocytose rituximab-opsonized leukemic targets more efficiently than m1 cells in vitro. J. Immunol. *182*, 4415–4422.

MacPhee, M., Chepenik, K.P., Liddell, R.A., Nelson, K.K., Siracusa, L.D., and Buchberg, A.M. (1995). The secretory phospholipase A_2 gene is a candidate for the *Mom1* locus, a major modifier of Apc^{Min}-induced intestinal neoplasia. Cell *81*, 957–966.

Miki, Y., Yamamoto, K., Taketomi, Y., Sato, H., Shimo, K., Kobayashi, T., Ishikawa, Y., Ishii, T., Nakanishi, H., Ikeda, K., et al. (2013). Lymphoid tissue phospholipase A_2 group IID resolves contact hypersensitivity by driving antiinflammatory lipid mediators. J. Exp. Med. *210*, 1217–1234.

Miller, A.M., Asquith, D.L., Hueber, A.J., Anderson, L.A., Holmes, W.M., McKenzie, A.N., Xu, D., Sattar, N., McInnes, I.B., and Liew, F.Y. (2010). Interleukin-33 induces protective effects in adipose tissue inflammation during obesity in mice. Circ. Res. *107*, 650–658.

Murakami, M., Taketomi, Y., Miki, Y., Sato, H., Hirabayashi, T., and Yamamoto, K. (2011). Recent progress in phospholipase A_2 research: from cells to animals to humans. Prog. Lipid Res. *50*, 152–192.

Namgaladze, D., Morbitzer, D., von Knethen, A., and Brüne, B. (2010). Phospholipase A_2-modified low-density lipoprotein activates macrophage peroxisome proliferator-activated receptors. Arterioscler. Thromb. Vasc. Biol. *30*, 313–320.

Odegaard, J.I., and Chawla, A. (2013). The immune system as a sensor of the metabolic state. Immunity *38*, 644–654.

Oh, D.Y., and Olefsky, J.M. (2012). ω 3 fatty acids and GPR120. Cell Metab. *15*, 564–565.

Ohtsuki, M., Taketomi, Y., Arata, S., Masuda, S., Ishikawa, Y., Ishii, T., Takanezawa, Y., Aoki, J., Arai, H., Yamamoto, K., et al. (2006). Transgenic expression of group V, but not group X, secreted phospholipase A_2 in mice leads to neonatal lethality because of lung dysfunction. J. Biol. Chem. *281*, 36420–36433.

Ozcan, U., Yilmaz, E., Ozcan, L., Furuhashi, M., Vaillancourt, E., Smith, R.O., Görgün, C.Z., and Hotamisligil, G.S. (2006). Chemical chaperones reduce ER stress and restore glucose homeostasis in a mouse model of type 2 diabetes. Science *313*, 1137–1140.

Pelleymounter, M.A., Cullen, M.J., Baker, M.B., Hecht, R., Winters, D., Boone, T., and Collins, F. (1995). Effects of the obese gene product on body weight regulation in *ob/ob* mice. Science *269*, 540–543.

Pettersson, C., Fogelstrand, L., Rosengren, B., Ståhlman, S., Hurt-Camejo, E., Fagerberg, B., and Wiklund, O. (2008). Increased lipolysis by secretory phospholipase A($_2$) group V of lipoproteins in diabetic dyslipidaemia. J. Intern. Med. *264*, 155–165.

Pruzanski, W., Lambeau, L., Lazdunsky, M., Cho, W., Kopilov, J., and Kuksis, A. (2005). Differential hydrolysis of molecular species of lipoprotein phosphatidylcholine by groups IIA, V and X secretory phospholipases A_2. Biochim. Biophys. Acta *1736*, 38–50.

Satake, Y., Diaz, B.L., Balestrieri, B., Lam, B.K., Kanaoka, Y., Grusby, M.J., and Arm, J.P. (2004). Role of group V phospholipase A_2 in zymosan-induced eicosanoid generation and vascular permeability revealed by targeted gene disruption. J. Biol. Chem. *279*, 16488–16494.

Sato, H., Kato, R., Isogai, Y., Saka, G., Ohtsuki, M., Taketomi, Y., Yamamoto, K., Tsutsumi, K., Yamada, J., Masuda, S., et al. (2008). Analyses of group III secreted phospholipase A_2 transgenic mice reveal potential participation of this enzyme in plasma lipoprotein modification, macrophage foam cell formation, and atherosclerosis. J. Biol. Chem. *283*, 33483–33497.

Sato, H., Taketomi, Y., Isogai, Y., Miki, Y., Yamamoto, K., Masuda, S., Hosono, T., Arata, S., Ishikawa, Y., Ishii, T., et al. (2010). Group III secreted phospholipase A_2 regulates epididymal sperm maturation and fertility in mice. J. Clin. Invest. *120*, 1400–1414.

Sergouniotis, P.I., Davidson, A.E., Mackay, D.S., Lenassi, E., Li, Z., Robson, A.G., Yang, X., Kam, J.H., Isaacs, T.W., Holder, G.E., et al. (2011). Biallelic mutations in PLA2G5, encoding group V phospholipase A_2, cause benign fleck retina. Am. J. Hum. Genet. *89*, 782–791.

Spite, M., Clària, J., and Serhan, C.N. (2014). Resolvins, specialized proresolving lipid mediators, and their potential roles in metabolic diseases. Cell Metab. *19*, 21–36.

Su, X., Mancuso, D.J., Bickel, P.E., Jenkins, C.M., and Gross, R.W. (2004). Small interfering RNA knockdown of calcium-independent phospholipases A_2 β or γ inhibits the hormone-induced differentiation of 3T3-L1 preadipocytes. J. Biol. Chem. *279*, 21740–21748.

Suzuki, N., Ishizaki, J., Yokota, Y., Higashino, K., Ono, T., Ikeda, M., Fujii, N., Kawamoto, K., and Hanasaki, K. (2000). Structures, enzymatic properties, and expression of novel human and mouse secretory phospholipase $A_{(2)}$s. J. Biol. Chem. *275*, 5785–5793.

Taketomi, Y., Ueno, N., Kojima, T., Sato, H., Murase, R., Yamamoto, K., Tanaka, S., Sakanaka, M., Nakamura, M., Nishito, Y., et al. (2013). Mast cell maturation is driven via a group III phospholipase A_2-prostaglandin D_2-DP1 receptor paracrine axis. Nat. Immunol. *14*, 554–563.

Tian, C., Stokowski, R.P., Kershenobich, D., Ballinger, D.G., and Hinds, D.A. (2010). Variant in PNPLA3 is associated with alcoholic liver disease. Nat. Genet. *42*, 21–23.

Titos, E., Rius, B., González-Périz, A., López-Vicario, C., Morán-Salvador, E., Martínez-Clemente, M., Arroyo, V., and Clària, J. (2011). Resolvin D1 and its precursor docosahexaenoic acid promote resolution of adipose tissue inflammation by eliciting macrophage polarization toward an M2-like phenotype. J. Immunol. *187*, 5408–5418.

Valentin, E., Ghomashchi, F., Gelb, M.H., Lazdunski, M., and Lambeau, G. (1999). On the diversity of secreted phospholipases $A_{(2)}$. Cloning, tissue distribution, and functional expression of two novel mouse group II enzymes. J. Biol. Chem. *274*, 31195–31202.

Wang, H., Astarita, G., Taussig, M.D., Bharadwaj, K.G., DiPatrizio, N.V., Nave, K.A., Piomelli, D., Goldberg, I.J., and Eckel, R.H. (2011). Deficiency of lipoprotein lipase in neurons modifies the regulation of energy balance and leads to obesity. Cell Metab. *13*, 105–113.

Wootton, P.T., Arora, N.L., Drenos, F., Thompson, S.R., Cooper, J.A., Stephens, J.W., Hurel, S.J., Hurt-Camejo, E., Wiklund, O., Humphries, S.E., and Talmud, P.J. (2007). Tagging SNP haplotype analysis of the secretory PLA_2-V gene, PLA2G5, shows strong association with LDL and oxLDL levels, suggesting functional distinction from sPLA$_2$-IIA: results from the UDACS study. Hum. Mol. Genet. *16*, 1437–1444.

Yamamoto, T., and Ryan, R.O. (2007). Anionic phospholipids inhibit apolipoprotein E—low-density lipoprotein receptor interactions. Biochem. Biophys. Res. Commun. *354*, 820–824.